EFFECT OF DEFECT ON THE MECHANICAL PROPERTIES OF NANOPOROUS TWO-DIMENSIONAL BOROPHENE MEMBRANES

Thien-Kim Huynh, Le-Hung-Toan Do*

The University of Danang - University of Science and Technology, Vietnam

*Corresponding author: dlhtoan@dut.udn.vn

(Received: December 13, 2025; Revised: January 21, 2026; Accepted: March 19, 2026)

DOI: 10.31130/ud-jst.2026.24(3).714

Abstract - Borophene, a two-dimensional material with remarkable electrochemical and mechanical potential, has attracted increasing attention for advanced nanoscale applications. This makes it crucial to investigate and determine how defects affect the mechanical characteristics of nanoporous 2D borophene nanosheets. This study discovers the width and quantity of vacancy defects on the borophene surface based on its structure. The results of this study will include parameters such as strain and stress curve diagrams, Young's modulus coefficients, and various maximum strength. In this work, the mechanical behavior of borophene monolayer films containing vacancy defects under uniaxial tensile conditions is studied using molecular dynamics simulation. The effect of vacancy defect widths and quantity to fracture behavior has been divided into two scenarios under uniaxial tension were investigated in both armchair (y) – zigzag (x) orientations.

Key words - Borophene; defect; strain; stress; molecular dynamics simulation.

1. Introduction

Since the discovery of graphene in 2004 [1], research on ultra-thin materials, namely nanomaterials, has expanded rapidly because of their promising applications in photocatalysis, electrocatalysis, biomaterials, and energy storage. In recent years, many in-depth studies have focused on two-dimensional (2D) materials, particularly in the fields of electronics, optoelectronics, sensors, and energy storage systems. The versatility of these materials, especially when the size and morphology of vacancy defects can be adjusted, has attracted the attention of materials scientists due to their unique interactions with various external agents [2–4].

Since the first study on the synthesis method of borophene in 2015 by A. J. Mannix et al. [5], borophene has rapidly become a major focus of research in the field of two-dimensional materials. Two main crystalline phases of this material have been identified: $\delta 6$ borophene – a buckled structure without vacancies [5] and $\beta 12$ borophene – a planar structure with distributed vacancies [6]. One of the remarkable features of borophene is the presence of a negative Poisson's ratio, accompanied by highly anisotropic mechanical behavior and thermal conductivity [7, 8–11], with a Young's modulus lower than that of graphene along the zigzag (x) direction but higher along the armchair (y) direction [12]. Owing to its highly anisotropic crystal structure, many studies have examined its electronic, mechanical, thermal, and optical behaviors [13–15].

Although the effects of defects and porosity on the mechanical properties of borophene have been investigated in several previous studies, the objectives and scope of analysis of those works remain significantly different from those presented in this study. Specifically, in the work of Zhou et al. [9], the research primarily focused on the establishment and evaluation of the interatomic potential function, together with the influence of loading conditions and temperature on the mechanical behavior of pristine borophene sheets (without defects). In that study, geometric factors related to vacancy defects, including defect width and defect number, were not comprehensively investigated. Meanwhile, the study by Pham et al. [11] focused on evaluating the roles of porosity and temperature in the mechanical behavior and thermal conductivity of borophene films. In that work, defects were described through the ratio of removed atoms to the total initial number of atoms, i.e., a global quantity. This approach does not clearly reveal the distinct role of defect geometry, particularly the width of vacancy defects, as well as the number of independent defect regions in the structure.

In contrast, the distinction and core novelty of the present study lie in the comprehensive evaluation of the effects of vacancy defect width and defect number on the mechanical properties of 2D borophene under uniaxial tension along the two characteristic directions, namely zigzag and armchair. Although these parameters play a key role in controlling stress distribution, fracture deformation processes, and the mechanical anisotropy of 2D sheets, they have not yet been separately and thoroughly investigated in the previously mentioned studies.

Despite its potential, the mechanical response of monolayer borophene containing uniformly distributed vacancy defects has not yet been fully evaluated and analyzed. In particular, the effects of the width and number of vacancy defects under uniaxial tensile loading have not been completely clarified. Therefore, this study employs molecular dynamics simulations to explore and evaluate how vacancy defects affect the Young's modulus and ultimate strength of borophene sheets subjected to uniaxial tension along both the zigzag and armchair directions. Examining and analyzing these defect forms, especially by considering differences in defect length, width, and number, is essential for a deeper assessment of the behavior and potential applications of 2D materials, particularly borophene.

This study primarily focuses on two key geometric characteristics of vacancy defects, namely their size (length and width) and quantity. Previous studies published in The

University of Danang - Journal of Science and Technology have investigated the mechanical behavior of two-dimensional materials from different perspectives. For example, Pham et al. [16] examined the effects of defect geometry, particularly defect length and orientation, on the tensile properties of nanoporous h-BN, demonstrating that stress concentration around defect regions significantly degrades mechanical performance. In addition, other studies, such as the work on GeO_2 and SnO_2 (XO_2) monolayer materials [17], have employed first-principles methods to evaluate both mechanical and electronic properties, highlighting the diversity of computational approaches applied to two-dimensional systems. However, these investigations mainly focus on specific material systems or individual factors, and often utilize different simulation techniques. In contrast, the present study adopts molecular dynamics simulations to systematically investigate the combined effects of defect size and quantity on the mechanical behavior of borophene. This approach aims to provide a more comprehensive understanding of defect-induced mechanical responses and to complement existing studies across different materials and computational frameworks.

Regarding the shape and distribution of defects, this work is idealized in terms of modeling. This approach is intentionally chosen to isolate and clarify the role of vacancy defects in the mechanical properties of the material. In reality borophene structures, defects often exist with random shapes and positions, making it very difficult to reproduce the exact experimental structures in simulations. Therefore, constructing and using defect models with controlled geometry is a common and necessary method for understanding the fundamental mechanical mechanisms. Furthermore, with the continued advancement of fabrication technologies and defect control techniques at the nanoscale [18], controlling defect geometry and density to optimize the mechanical properties of materials is becoming increasingly feasible and practically meaningful.

Moreover, more detailed studies on the mechanical behavior of monolayer borophene containing vacancy defects are needed to clearly determine how these imperfections affect the performance of the material.

2. Method

An ideal 2D borophene sheet is the starting point for this investigation. Figure 1 illustrates borophene with a highly anisotropic crystal structure, whose unit cell is rectangular. Based on the crystal structure in the Z–X and Z–Y planes, the structure exhibits corrugation lines along the x-direction, whereas no corrugation lines are observed along the y-direction. The fully optimized lattice parameters of free-standing borophene are a = 0.29 nm and b = 0.16 nm. These parameters were reported by R. C. Xiao et al. in 2016 [19].

This study employs molecular dynamics simulations to examine the effects of vacancy defects on the mechanical properties of 2D borophene nanosheets. To better understand the load-bearing capacity of the material, a monolayer borophene model was constructed to examine its behavior under uniaxial tensile loading. As shown in Figure 1, the simulations were performed on borophene structures with different numbers and widths of vacancy defects. The simulation model has in-plane dimensions of 25 × 25 nm in the X–Y coordinates.

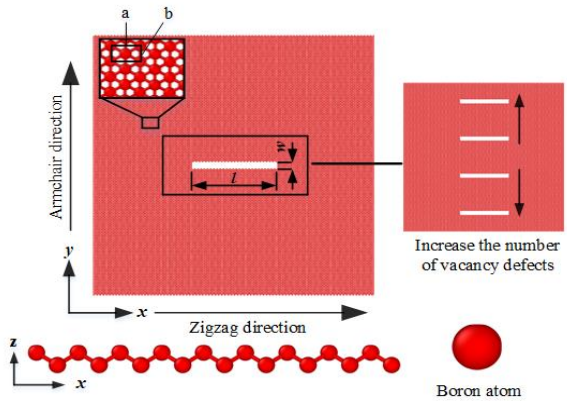

Figure 1. *Atomic configurations (crystal structure and atomic lattice) of monolayer borophene sheets with different widths and numbers of vacancy defects placed at the center of the sheet. These configurations were prepared to analyze their mechanical behavior under uniaxial tension. The zigzag/armchair directions of the material are illustrated in the Z–X and Z–Y planes, respectively*

In all molecular dynamics simulations, periodic boundary conditions (PBC) were applied in all three spatial directions (X, Y, and Z) to model an infinitely large borophene sheet in the plane. To prevent interactions between borophene sheets when periodic boundary conditions were applied along the z-direction, a vacuum space of 5 nm was created above and below the sheet along the z-direction, as described in Figure 2(a–b). Periodic boundary conditions were applied to the system in all three spatial directions. The system employed the conjugate gradient (CG) energy minimization method to eliminate residual stresses generated during the construction of the initial model before the tensile test, thereby allowing the structure to reach an equilibrium state. The simulation time step was set to 1 fs. The energy of the system under dynamic conditions was minimized in the NVE ensemble (constant volume and energy) at room temperature 300 K for 100 ps. After that, the system was simulated in the NPT ensemble (constant pressure and temperature) for 50 ps at the same temperature to minimize any abnormal residual stresses remaining in the structure. Subsequently, uniaxial tension was applied at a constant strain rate of 10^9 s^{-1}, a value commonly used in molecular dynamics simulations. The loading process was conducted in the NPT ensemble with a simulation time step of 1 fs. During uniaxial stretching along the x-direction, the Nosé–Hoover barostat was used to maintain zero pressure along the y-direction. Similarly, during uniaxial stretching along the y-direction, the pressure was maintained at zero along the x-direction. This setup ensures pure uniaxial tension conditions and limits undesired constraint effects from the directions perpendicular to the loading direction.

A high strain rate may affect the fracture behavior of borophene sheets in uniaxial tensile simulations.

As the strain rate increases, atoms have less time to respond to the tensile force, resulting in bond breaking occurring more simultaneously and being distributed more uniformly. Therefore, simulations at high strain rates often yield higher strength and fracture strain values than cases with lower strain rates. This trend has been reported in many previous molecular dynamics simulation studies [20–21].

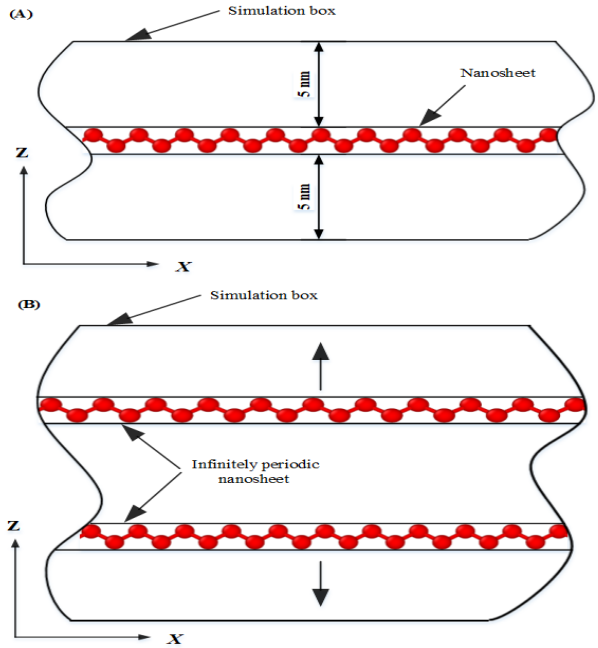

Figure 2. *Description of the periodic boundary conditions (PBC). (a) A vacuum space of 5 nm is introduced along the z-direction between the upper and lower surfaces of the borophene sheet. (b) The borophene sheet repeats periodically and infinitely along the z-direction*

To ensure consistency and facilitate comparison among defect configurations, all simulations in this study were performed at a fixed strain rate of 1×10^9 s^{-1}. Although the absolute values of mechanical quantities may depend on the strain rate, the use of a constant value ensures that the observed trends in this work primarily reflect the effects of vacancy defect width and number, rather than the influence of loading conditions.

In molecular dynamics simulation studies, strain rates in the range of 1×10^8 s^{-1} to 1×10^9 s^{-1} are commonly used; therefore, the value adopted in this study is reasonable and consistent with the published literature.

In this work, a "vacancy defect" is defined as an extended defective region created by removing a group of bonded boron atoms, thereby forming a continuous void region with a defined length and width in the plane of the borophene sheet. The geometric dimensions of the defect region were selected in a controlled manner to allow a comprehensive investigation of the effects of defect width and number on the mechanical behaviors of borophene nanosheets under uniaxial tension.

From the vacancy defects located at the center of the model, two cases were generated, including: variation in defect width (w), and variation in the number of vacancy defects (n).

The internal stress was recorded throughout the tensile process to analyze the mechanical behaviors of nanoporous monolayer borophene sheets. At the atomic level, the stress components were determined based on the Virial theorem [22], which provides a theoretical framework for relating atomic interactions to macroscopic stress quantities.

$$\sigma = \frac{1}{V}\sum_{a\in V}\left[-m_a v_a \otimes v_a + \frac{1}{2}\sum_{a\neq b}(r_{ab}\otimes F_{ab})\right] \quad (1)$$

where m_a and v_a represent the mass and velocity vectors, respectively, of atom a in the borophene structure. V denotes the volume of the structure, considering a thickness of t = 0.48 nm [21]. The parameter r_{ab} denotes the distance vector between atoms a and b, while the symbol $\otimes$ in this expression denotes the tensor product of two vectors. In addition, F_{ab} corresponds to the force vector acting between atoms a and b.

The von Mises stress, σ_{von} is defined by the following expression [23]:

$$\sigma_{von}^2 = \frac{1}{2}\begin{bmatrix}(\sigma_{xx}-\sigma_{yy})^2+(\sigma_{yy}-\sigma_{zz})^2\\+(\sigma_{zz}-\sigma_{xx})^2+6(\sigma_{xy}^2+\sigma_{yz}^2+\sigma_{zx}^2)\end{bmatrix} \quad (2)$$

where, σ_{xx}, σ_{yy}, σ_{zz}, σ_{xy}, σ_{yz} and σ_{zx} are the six components of the atomic stress tensor.

The engineering strain is described by the following equation [11]:

$$\varepsilon = \frac{L-L_0}{L_0} \quad (3)$$

where L_0 is assumed to be the initial dimension of the structure and L is the dimension of the structure after deformation.

All molecular dynamics simulations were performed using the LAMMPS software package [24], and the obtained data - including the deformation and fracture processes - were analyzed and visualized using OVITO [25]. In this model, the interactions between boron atoms in the borophene sheet were represented using the Stillinger–Weber (SW) potential [26].

3. Results and discussion

In this work, the investigation is divided into two parts, including the examination of the effects of defect width and defect number in borophene nanosheets on their mechanical properties.

3.1. Effect of defect width

In terms of geometric description, the length of a vacancy defect is defined as the size of the defect region along the X-direction, whereas the width of a vacancy defect corresponds to the size of the defect region along the Y-direction. Increasing the length or width of a vacancy defect means removing an additional group of bonded boron atoms along the X- or Y-direction.

This study focuses on systematically analyzing the effects of vacancy defect width and vacancy defect number on the mechanical properties of borophene sheets under uniaxial tension along the X- and Y-directions. Since the effect of vacancy defect length has been reported in previous scientific publications [21], this factor is beyond the scope of the present work. Instead, the study focuses on

investigating and evaluating the distinct roles of defect width and defect density in the mechanical behavior and fracture mechanism of the material.

To investigate the effect of defect width on the mechanical behavior of borophene nanosheets under uniaxial tensile testing, a series of molecular dynamics (MD) simulations was conducted on pristine borophene sheets and borophene sheets with defect widths ranging from 1.0 nm đến 2.6 nm along both the armchair and zigzag directions, at room temperature 300 K and a strain rate of 1×10^{9} s^{-1}. The outputs of these simulations include images of stress distribution and fracture behavior, while also providing parameters for the stress–strain curves, maximum stress (ultimate strength), and Young's modulus of the material.

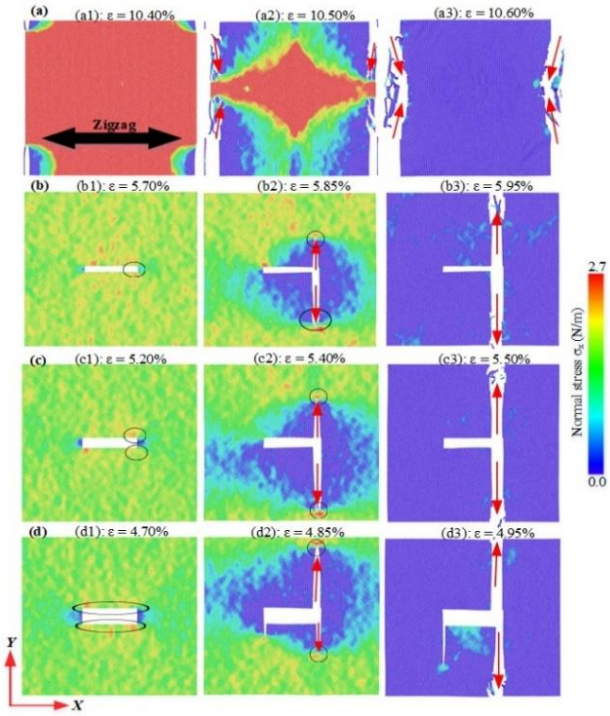

Figure 3. *Stress distribution and deformation behavior during uniaxial tensile loading along the x-direction (zigzag) of monolayer borophene sheets at 300 K for vacancy defects with the same length of 7.6 nm but but different widths: (a) pristine model, (b) 1.0 nm, (c) 1.6 nm, and (d) 2.6 nm*

The fracture deformation process and stress distribution under uniaxial tension along the x-direction (zigzag) of monolayer borophene sheets are illustrated in Figure 3. The tensile tests were carried out at 300 K for vacancy defects with the same length of 7.6 nm but different widths: (b) 1.0 nm, (c) 1.6 nm, (d) 2.6 nm compared with the pristine sheet (a). Similar to the previous results, as the strain increases, the stress in the sheet increases, and high-stress regions are concentrated along the two side edges of the vacancy defect. As the strain value increases during stretching along the x-direction, the normal stress value σ_x also increases. As the strain continues to increase, cracks begin to form and rapidly propagate in the direction perpendicular to the loading direction, as indicated by the red arrows (the red arrows conventionally represent fracture cracks along the armchair direction). The results show that as the defect width increases, both the ultimate strength (maximum stress) and the fracture strain decrease.

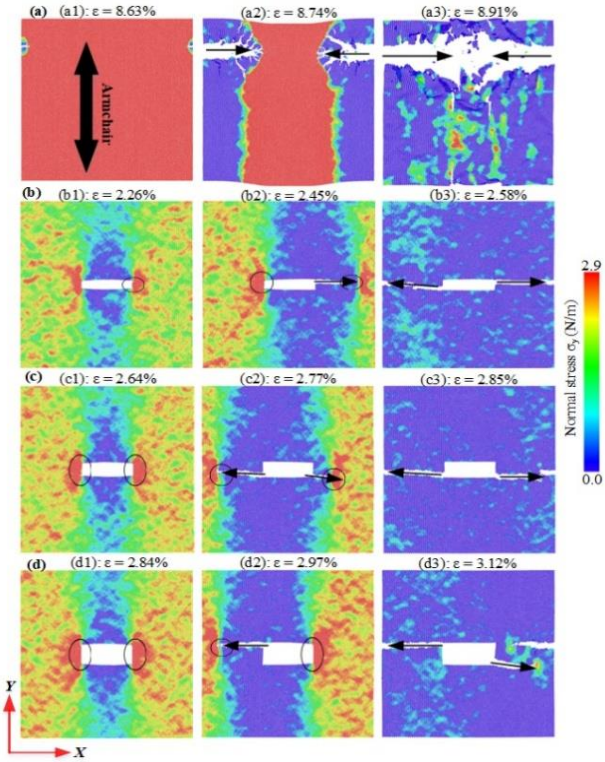

Figure 4. *Stress distribution and deformation behavior during uniaxial tensile loading along the y-direction (armchair) of monolayer borophene sheets at 300 K for vacancy defects with the same length of 7.6 nm but different widths: (a) pristine model, (b) 1.0 nm, (c) 1.6 nm, and (d) 2.6 nm*

Figure 4 illustrates the fracture deformation process of monolayer borophene sheets under uniaxial tension along the y-direction (armchair) at a temperature of 300 K. The analysis focuses on three different vacancy defect widths, each having the same length of 7.6 nm but different widths of (b) 1.0 nm, (c) 1.6 nm and (d) 2.6 nm, compared with the pristine sheet (a). The color-coded stress bar provides insight into the mechanical behavior of borophene sheets under different widths. At strain values of 8.63%; 2.26%; 2.64% and 2.84% in each case, cracks begin to form in the borophene sheets. These cracks propagate rapidly, leading to complete failure of the sheets at strain values of 8.91%; 2.58%; 2.85% and 3.12%, respectively. This phenomenon can be explained based on the relationship between vacancy defect geometry and the crack propagation mechanism. When the width of the vacancy defect increases along the Y-direction, that is, parallel to the armchair loading direction, the defect region expands along the loading direction. Under uniaxial tension along the Y-direction, cracks tend to initiate and propagate in the direction perpendicular to the loading direction, i.e., along the X-direction, causing stress concentration along the two side edges of the vacancy defect. The increase in vacancy defect width enlarges the defect boundary size parallel to the loading direction, thereby allowing the stress to be redistributed over a broader region instead of being locally concentrated at the defect tips. As a result, the

borophene sheet can reach higher maximum stress and fracture strain values before complete failure occurs, although it still remains weaker than the pristine sheet.

Notably, the pristine borophene sheet (without vacancy defects) exhibits the highest fracture strain. When vacancy defects are introduced into the structure, the fracture strain decreases significantly, indicating that the presence of vacancy defects strongly affects the deformability and mechanical properties of the material. This result emphasizes the dominant role of vacancy defects in degrading the deformation capacity of two-dimensional borophene sheets.

In addition, the dependence of fracture strain on the loading direction is also clearly observed. When the borophene sheet is stretched along the armchair direction (y), the fracture strain gradually increases as the vacancy defect width increases. In contrast, in the case of stretching along the zigzag direction (x), the fracture strain decreases from 5.95% to 4.95% as the defect width increases from 1.0 nm to 2.6 nm. This difference indicates that, in addition to the effect of vacancy defect size, the uniaxial loading direction plays an important role in governing the mechanical behavior of borophene sheets.

Figure 5 presents the tensile stress–strain relationship of monolayer borophene sheets at 300 K in relation to variations in defect width while maintaining a constant defect length of 7.6 nm. The curves illustrate the stress–strain behavior along two crystallographic directions, armchair and zigzag, under uniaxial tension with different vacancy defect widths. The stress–strain curves clearly distinguish the different defect widths along the zigzag direction. When the vacancy defect width increases in the direction perpendicular to the loading direction, the ultimate strength of the nanosheet decreases, as shown in Figure 5(a). In contrast, under uniaxial tension along the armchair direction, the length of the vacancy defect in the direction perpendicular to the loading direction remains unchanged, but due to the increase in defect width along the loading direction, the maximum stress and fracture strain increase, as shown in Figure 5(b). This indicates that defect width significantly affects the mechanical properties of 2D sheets; moreover, the effect of defect width depends on the direction of uniaxial stretching. In both directions (zigzag and armchair), after reaching the maximum stress, the stress decreases abruptly, signaling the onset of mechanical failure.

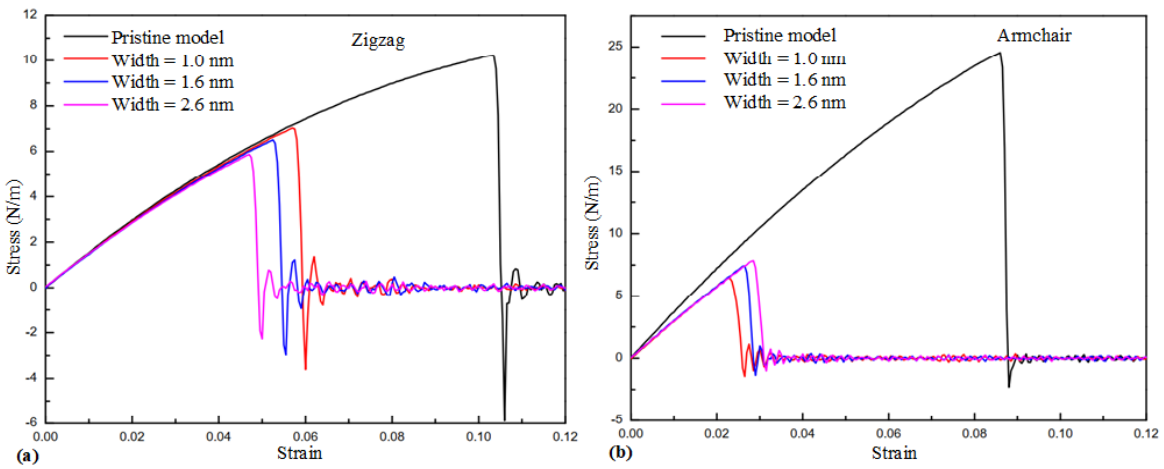

Figure 5. *Stress–strain curves of borophene sheets at room temperature 300K with varying defect width while maintaining the vacancy defect length at 7.6 nm compared with the defect-free model, under uniaxial tension along the (a) zigzag and (b) armchair directions*

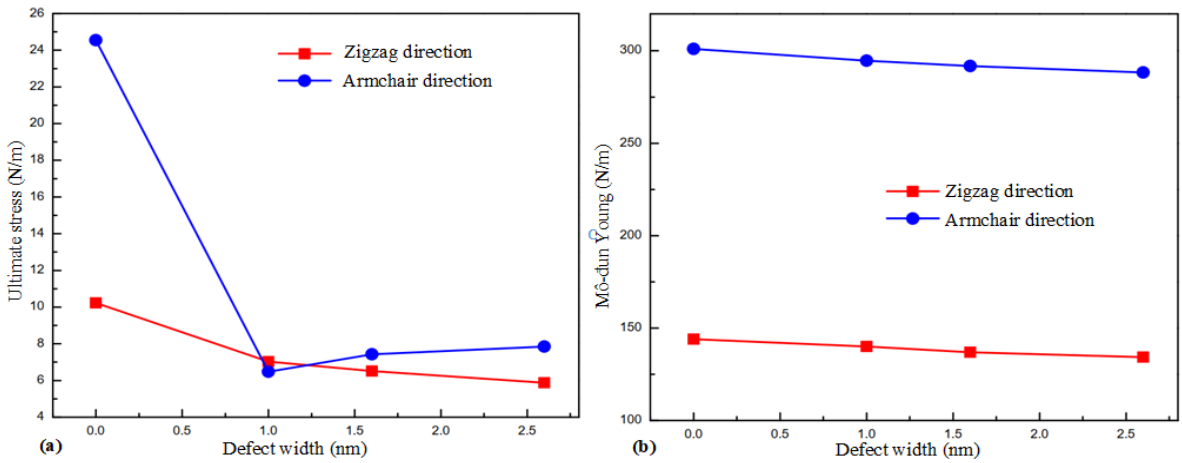

Figure 6. *Dependence of vacancy defect width on (a) maximum stress and (b) Young's modulus of monolayer borophene sheets at 300K under uniaxial tension along the X (zigzag) and Y (armchair) directions*

Table 1. *Comparison of the properties of borophene nanosheets in this study with those reported in a previous study.*

	Young's modulus (N/m)	Fracture strain %	Ultimate stress (N/m)	Temperature	Reference
Borophene	~140 (zigzag)	~10.0	~10.2	300 K	This work
	~348 (armchair)	~8.9	~25.0	300 K	
Borophene	~151 (zigzag)	~11.0	~10.0	300 K	V.T. Pham et al. [11]
	~370 (armchair)	~9.0	~24.5	300 K	
h-BN	~225 (armchair)	~32.6	~40.5	300 K	V.T. Pham et al. [16]
	~220 (zigzag)	~25.5	~36.0	300 K	

Figure 6 illustrates the effect of vacancy defect width on both the maximum stress (a) and Young's modulus (b) of monolayer borophene under uniaxial tension. Figure 6(a) shows that the defect-free sheet has the highest maximum stress value, whereas when vacancy defects appear in the nanosheet, the maximum stress decreases sharply. Moreover, if the vacancy defect width increases, the fracture strength and fracture strain decrease under uniaxial tension along the zigzag direction but increase under uniaxial tension along the armchair direction. Consistent with the stress–strain curves, Young's modulus at different defect widths is determined in Figure 6(b), where the Young's modulus value decreases linearly in both cases. In general, under uniaxial tension along the armchair direction, the highest maximum stress values are observed, and defect width generally reduces the maximum stress.

Table 1 presents a comparison of the Young's modulus, tensile strength, and fracture strain values of defect-free borophene sheets from this study and the previous study. The findings indicate that the values obtained in this study are in agreement with those reported in the previous work. This consistency suggests that the findings regarding the effects of vacancy defects on the mechanical properties of borophene sheets are reliable and may serve as a reference for future research.

3.2. Effect of defect quantity

Figure 7 presents the fracture behavior of a monolayer borophene nanosheet under uniaxial tension along the zigzag direction (x-direction) at 300 K. The color bar represents the distribution of normal stress in units of N/m, with atomic stresses displayed in the sheet.

The results in Figure 7 show how different numbers of vacancy defects affect the stress distribution and crack propagation under uniaxial tension along the zigzag direction. As the strain increases, stress concentrates at the edges of the vacancy defects, leading to the onset of fracture. Figure 7(a–d) shows that at strain values of 6.80%; 7.05%; 5.90% and 6.40%, cracks begin to form in the nanosheets. The nanosheets fracture completely when the strain reaches 7.05%; 7.30%; 6.15% and 6.65% for 1, 2, 3, and 4 vacancy defects, respectively. The crack propagation path depends on the number of defects, with fracture tending to occur between or around the vacancy defects, and the cracks being perpendicular to the applied tensile load. As the number of defects increases, the fracture strain does not follow a definite trend when the sheet is stretched along the zigzag direction. Specifically, when the number of vacancy defects in the sheet increases from 1 to 2, the fracture strain increases, but when the number further increases to 3 vacancy defects, this value decreases significantly from 7.30% to 6.15%.

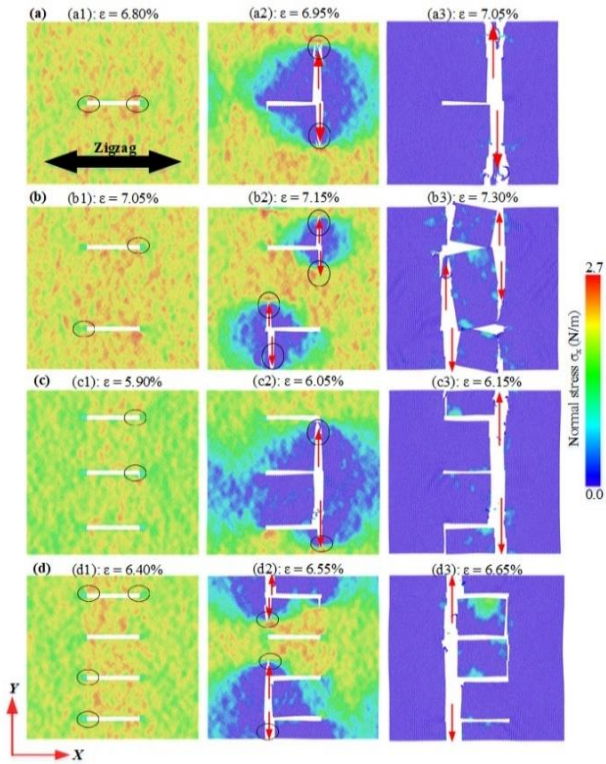

Figure 7. *Stress distribution and deformation behavior under uniaxial tension along the x-direction (zigzag) of monolayer orophene sheets at 300 K for different vacancy defects with the same length of 7.6 nm and width of 0.6 nm: (a) 1 vacancy defect, (b) 2 vacancy defects, (c) 3 vacancy defects, and (d) 4 vacancy defects*

Figure 8 presents a series of simulation snapshots showing the deformation behavior of a monolayer borophene nanosheet under uniaxial tension along the y-direction at 300 K. The figure illustrates how the number of vacancy defects in the sheet affects the stress distribution and failure behavior. The color bar beside the images represents the normal stress value in units of N/m. For 1, 2, 3, and 4 defects, cracks begin to form at strain levels of 2.30%; 3.04%; 3.57% and 4.08%, respectively. Similar to the case of varying defect width, increasing the number of vacancy defects along the Y-direction also significantly affects the failure mechanism of borophene sheets under uniaxial tension along the armchair direction. However, in this case, the governing mechanism arises not only from the geometry of each individual defect but also

from the interaction between neighboring defects. As the number of vacancy defects increases, the defects are arranged parallel to the loading direction, creating more potential stress concentration sites. For example, the observation in Figure 8(d) shows that the nanosheet with 4 vacancy defects has 8 stress-bearing regions when stretched along the armchair direction. Under loading along the Y-direction, cracks tend to propagate in the direction perpendicular to the loading direction (i.e., along the X-direction). The simultaneous presence of multiple defects causes crack initiation to no longer be governed by a single defect but to be distributed over multiple locations along the loading direction. Due to the competition among these crack initiation sites, stress is no longer strongly concentrated locally at a single defect boundary but is instead distributed over several different boundary regions. This slows down the propagation of the dominant crack and delays the formation of a crack extending across the entire sheet. As a result, the borophene sheet can reach higher maximum stress and fracture strain values before complete failure occurs.

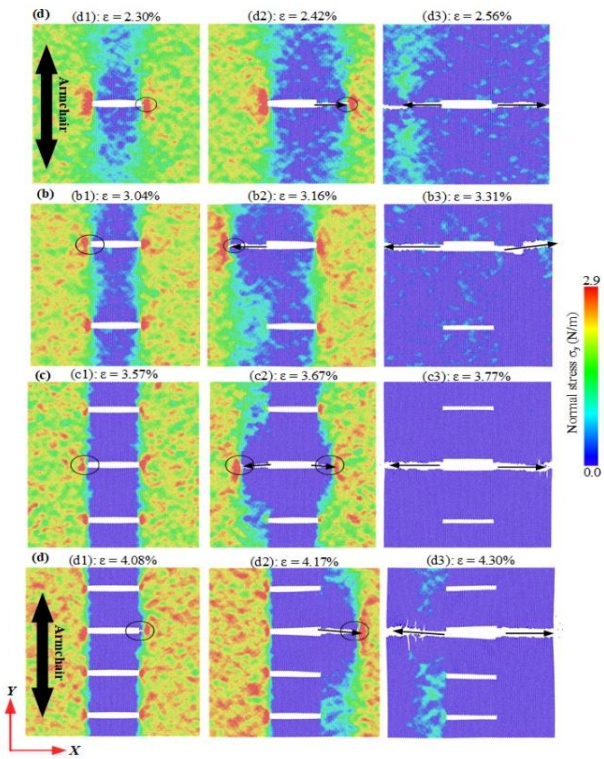

Figure 8. *Stress distribution and deformation behavior under uniaxial tension along the y-direction (armchair) of monolayer borophene sheets at 300 K for different vacancy defects with the same length of 7.6 nm and width of 0.6 nm: (a) 1 vacancy defect, (b) 2 vacancy defects, (c) 3 vacancy defects, and (d) 4 vacancy defects*

Vacancy defects in monolayer borophene significantly affect the stress distribution and crack initiation under uniaxial tensile stress. In all cases (1, 2, 3, and 4 vacancy defects), fracture initiates at the vacancy sites where stress concentration is highest. Stress begins to distribute around these vacancy defects at relatively low strain levels, and as the strain increases, these stress regions act as nucleation sites for crack formation. In contrast to the zigzag uniaxial tension case, in this case, as the number of defects increases, the fracture strain increases according to a specific trend under armchair loading, although the strain values are much smaller. Because the total projected length of the vacancy defects perpendicular to the y-direction (i.e., considering the horizontal projected length) is greater than the projected length perpendicular to the x-direction (considering the vertical projected length), the fracture strain is lower when the tensile load is applied along the y-direction than along the x-direction.

Figure 9 shows the stress–strain relationship of monolayer borophene sheets under uniaxial tension along the zigzag and armchair directions. Based on the observations in Figure 9(a–b), when the number of defects in the direction perpendicular to the loading direction increases, the mechanical properties of the material decrease. In contrast, when the number of vacancy defects along the loading direction increases (i.e., increasing the defect region along the Y-direction coinciding with the armchair loading direction), the mechanical properties increase.

Figure 10 shows the mechanical properties, including Young's modulus and maximum tensile strength, of monolayer borophene sheets at 300 K under uniaxial tension. The mechanical properties associated with the number of vacancy defects in the sheet are analyzed. For the case of uniaxial tension along the zigzag direction, the maximum stress decreases significantly as the number of vacancy defects increases, but not according to a definite rule; that is, when the number of vacancy defects increases from 1 to 2, the maximum stress increases, but when the defect regions increase to 3, this value decreases. In contrast, for uniaxial tension along the armchair direction, a clear and systematic increase in the maximum stress is observed as the number of vacancy defects increases, indicating improved tensile stress-bearing capacity when the number of defects increases along the uniaxial loading direction in the Y-direction (armchair).

Figure 10(b) illustrates the relationship between Young's modulus and the number of vacancy defects. The results show that Young's modulus decreases linearly as the number of defects increases in both uniaxial tensile tests along the two directions. These results provide insight into the mechanical response of borophene sheets under different loading conditions and vacancy defect structures, demonstrating the influence of defect formation on material strength.

Under uniaxial tension along the zigzag direction, Young's modulus gradually decreases as the number of vacancy defects increases from 1 to 4: 1 vacancy defect (144 N/m), 2 vacancy defects (139 N/m), 3 vacancy defects (136 N/m), and 4 vacancy defects with the lowest value of 133 N/m. Under tension along the armchair direction, the same order is maintained: 1 vacancy defect (295 N/m), 2 vacancy defects (272 N/m), 3 vacancy defects (262 N/m), and 4 vacancy defects (258 N/m). The results emphasize that the maximum stress is simultaneously affected by both the number of vacancy defects and the loading direction X and Y (armchair and zigzag). However, Young's modulus is affected only by the number of defects.

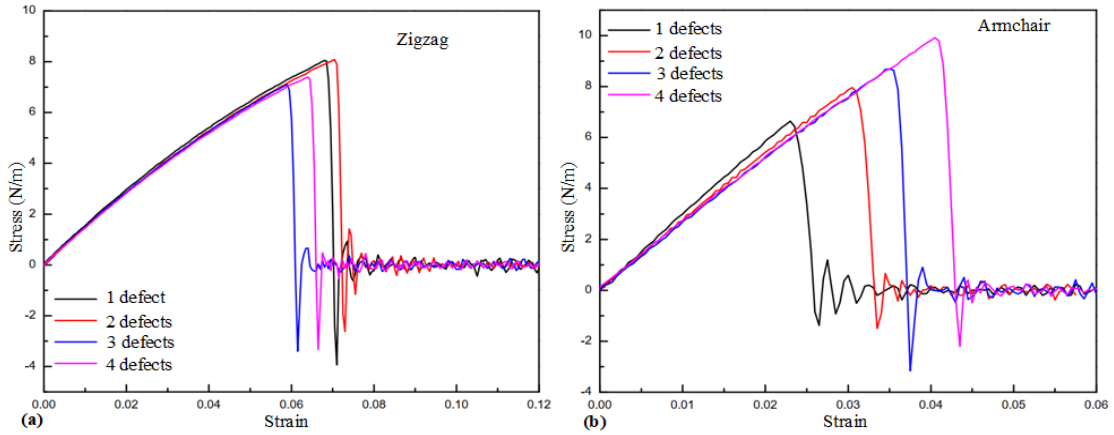

Figure 9. *Stress–strain curves of borophene sheets at room temperature 300K with varying numbers of vacancy defects with a length of 7.6 nm and a width of 0.6 nm under uniaxial tension along the (a) zigzag and (b) armchair directions*

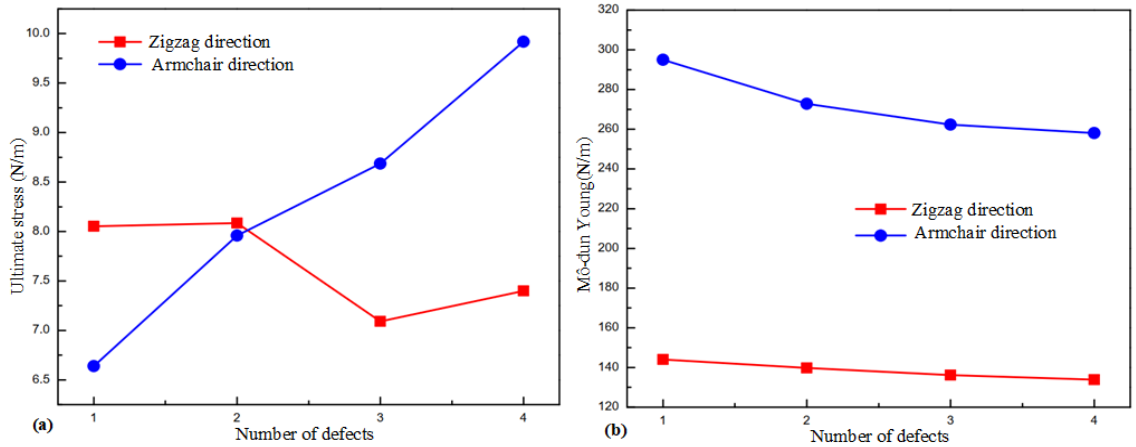

Figure 10. *Dependence of the number of vacancy defects on (a) maximum stress and (b) Young's modulus of monolayer borophene sheets at room temperature 300K under uniaxial tension along the X (zigzag) and Y (armchair) directions*

4. Conclusion

In this study, molecular dynamics simulations were used to investigate the mechanical properties of borophene under uniaxial tension along both the X (zigzag) and Y (armchair) directions. The effects of vacancy defect width and vacancy defect number on the fracture behavior of borophene nanosheets were examined. The results can be summarized as follows:

- The non-defect borophene sheet exhibits maximum stress values of 10.2 N/m and 25.0 N/m under uniaxial tension along the X and Y directions, respectively, at 300 K. Similarly, Young's modulus shows corresponding values consistent with those reflected by the maximum stress under tensile loading along the X and Y directions, regardless of the uniaxial tensile test. The maximum stress and Young's modulus of the 2D borophene sheet under uniaxial tension along the zigzag direction are always lower than those under tension along the armchair direction.

- In the uniaxial tensile test, increasing the vacancy defect width perpendicular to the loading direction reduces the fracture strain, maximum tensile strength, and Young's modulus. In contrast, the fracture strain and maximum stress increase when the defect width increases along the loading direction (i.e., increasing the defect size along the Y-direction, coinciding with the armchair stretching direction). This phenomenon can be explained as follows: when the vacancy defect width increases along the Y-direction, parallel to the armchair loading direction, the defect geometry changes the stress concentration and crack propagation mechanisms. Under uniaxial tension along the Y-direction, cracks tend to propagate in the perpendicular X-direction, while the extension of the defect along the loading direction allows stress to be redistributed over a broader boundary region.

- When the number of vacancy defects distributed perpendicular to the loading direction increases, the mechanical properties decrease. In contrast, when the loading direction (armchair direction) is parallel to the defect distribution (Y-direction), the mechanical properties increase. This indicates that the distribution of vacancy defects significantly affects the mechanical properties of the material. This phenomenon can be explained as follows: increasing the number of vacancy defects along the Y-direction, parallel to the armchair loading direction, changes the failure mechanism of the borophene sheet through the interaction among neighboring defects. Under uniaxial tension along

the Y-direction, cracks tend to propagate in the perpendicular X-direction, and the simultaneous presence of multiple defects creates multiple competing crack initiation sites. Due to the competition among these crack initiation sites, stress is no longer strongly concentrated locally at a single defect boundary, but is instead distributed over multiple boundary regions.

REFERENCES

[1] K. S. Novoselov *et al.*, "Electric Field Effect in Atomically Thin Carbon Films," *Science*, vol. 306, no. 5696, pp. 666-669, 2004.

[2] H. Wang *et al.*, "Porous Two-Dimensional Materials for Photocatalytic and Electrocatalytic Applications," *Matter*, vol. 2, no. 6, pp. 1377-1413, 2020.

[3] A. Mazinani *et al.*, "Comparative antibacterial activity of 2D materials coated on porous-titania," *Journal of Materials Chemistry B*, vol. 9, no. 32, pp. 6412-6424, 2021.

[4] J.S. Jang *et al.*, "2D Materials Decorated with Ultrathin and Porous Graphene Oxide for High Stability and Selective Surface Activity," *Advanced Materials*, vol. 32, no. 36, p. 2002723, 2020.

[5] A.J. Mannix *et al.*, "Synthesis of borophenes: Anisotropic, two-dimensional boron polymorphs," *Science*, vol. 350, no. 6267, pp. 1513-1516, 2015.

[6] B. Feng *et al.*, "Experimental realization of two-dimensional boron sheets," *Nature Chemistry*, vol. 8, no. 6, p. 563–568, 2016.

[7] V. T. Pham and T. H. Fang, "Anisotropic mechanical strength, negative Poisson's ratio and fracture mechanism of borophene with defects," *Thin Solid Films*, vol. 709, p. 138197, 2020.

[8] A. J. Mannix, Z. Zhang, N. P. Guisinger, B. I. Yakobson and M. C. Hersam, "Borophene as a prototype for synthetic 2D materials development," *Nature Nanotechnology*, vol. 13, no. 6, p. 444–450, 2018.

[9] Y.P. Zhou and J.W. Jiang, "Molecular dynamics simulations for mechanical properties of borophene: parameterization of valence force field model and Stillinger-Weber potential," *Scientific Reports*, vol. 7, no. 1, p. 45516, 2017.

[10] L. Yu, Q. Yan and A. Ruzsinszky, "Negative Poisson's ratio in 1T-type crystalline two-dimensional transition metal dichalcogenides," *Nature Communications*, vol. 8, no. 1, p. 15224, 2017.

[11] V.T. Pham and T.H. Fang, "Understanding porosity and temperature induced variabilities in interface, mechanical characteristics and thermal conductivity of borophene membranes," *Scientific Reports*, vol. 11, no. 1, p. 12123, 2021.

[12] H. Sun, Q. Li, and X.G. Wan, "First-principles study of thermal properties of borophene," *Physical Chemistry Chemical Physics*, vol. 18, no. 22, pp. 14927-14932, 2016.

[13] Z.Q. Wang, T.Y. Lu, H.Q. Wang, Y. P. Feng, and J.C. Zheng, "Review of borophene and its potential applications," *Frontiers of Physics*, vol. 14, no. 3, p. 33403, 2019.

[14] Y. Liu et al., "Stable and metallic borophene nanoribbons from first-principles calculations," *Journal of Materials Chemistry C*, vol. 4, no. 26, pp. 6380-6385, 2016.

[15] Z. Zhang, Y. Xie, Q. Peng and Y. Chen, "Phonon transport in single-layer boron nanoribbons," *Nanotechnology*, vol. 27, no. 44, p. 445703, 2016.

[16] V.T. Pham *et al.*, "Impact of defects on the mechanical characteristics of two-dimensional nanoporous boron nitride membranes," *The University of Danang - Journal of Science and Technology*, vol. 23, no. 9C, pp. 55-61, 2025.

[17] T.Q. Tran *et al.*, " Assessment of mechanical and electronic properties of XO_2 monolayer materials using first-principles method," *The University of Danang - Journal of Science and Technology*, vol. 23, no. 5A, pp. 7-12, 2025.

[18] S. Arabha, A.H. Akbarzadeh, and A. Rajabpour, "Engineered porous borophene with tunable anisotropic properties," *Composites Part B: Engineering*, vol. 200, pp. 108-260, 2020.

[19] R. C. Xiao, D. F. Shao, W. J. Lu, H. Y. Lv, J. Y. Li, and Y. P. Sun, "Enhanced superconductivity by strain and carrier-doping in borophene: A first principles prediction," *Applied Physics Letters*, vol. 109, no. 12, pp. 122-604, 2016.

[20] T. N. Vu, V. T. Pham, D. B. Luu, N. H. Tran, P. T. N. Nguyen, B. K. Nguyen, and Q. B. Tao, "Effect of nanopore on mechanical characteristics of indium selenide membrane," *Journal of the Brazilian Society of Mechanical Sciences and Engineering*, vol. 47, p. 83, 2025.

[21] Z. D. Sha *et al.*, "Temperature and strain-rate dependent mechanical properties of single-layer borophene," *Extreme Mechanics Letters*, vol. 19, pp. 39-45, 2018.

[22] D. Wang *et al.*, "Von Mises Stress in Chemical-Mechanical Polishing Processes," *Journal of The Electrochemical Society*, vol. 144, no. 3, p. 1121, 1997.

[23] N. Liu *et al.*, "Abnormality in fracture strength of polycrystalline silicene," *2D Materials*, vol. 3, no. 3, p. 035008, 2016.

[24] S. Plimpton, "Fast Parallel Algorithms for Short-Range Molecular Dynamics," *Journal of Computational Physics*, vol. 117, no. 1, pp. 1-19, 1995.

[25] A. Stukowski, "Visualization and analysis of atomistic simulation data with OVITO–the Open Visualization Tool," *Modelling and Simulation in Materials Science and Engineering*, vol. 18, no. 1, p. 015012, 2009.

[26] J. W. Jiang and Y. P. Zhou, "Parameterization of Stillinger-Weber Potential for Two-Dimensional Atomic Crystals," *Materials Science*, p. 1704.03147, 2017.